第 34 卷第 3 期
2015 年 6 月

红 外 与 毫 米 波 学 报
J. Infrared Millim. Waves

Vol. 34, No. 3
June,2015

文章编号: 1001 - 9014(2015)03 - 0271 - 05

DOI:10.11972/j.issn.1001 - 9014.2015.03.003

Improved design for low-sidelobe non-resonant slotted waveguide antenna

ZHAO De-Shuang*, LIU Chuan-Kai, WANG Bing-Zhong

(School of Physical Electronics, University of Electronic Science and Technology of China, Chengdu 610054, China)

Abstract: For fast design of millimeter-wave non-resonant slotted waveguide antennas (SWAs) with more accuracy, an improved analytical method is presented by introducing a modified factor into the traditional Stevenson's formula. The modified factor can greatly improve analytical calculation accuracy of slot displacement of longitudinal shunt slots cut in the broad face of a waveguide. Generally, the traditional Stevenson's formula is valid for only narrow slots of a length-to-width ratio of 10∶1. However, the proposed method allows for fast design of millimeter-wave SWAs of very low-sidelobe levels and wide slots of an approximately 4∶1 length-to-width ratio. A theoretical explanation of the modification was provided. With the improved method, a prototype of non-resonant SWAs operating in 60 GHz band was designed and fabricated. The measured gain and sidelobe level are 14.8 dB and −25 dB. Good agreement between the simulation results and measured data indicate the effectiveness of this improved method.

Key words: millimeter-wave, slotted waveguide antenna, Stevenson's formula, Taylor distribution

PACS: 84.40.Ba, 41.20.-q

毫米波段非谐振型低副瓣波导缝隙天线的改进型设计方法

赵德双*, 刘传凯, 王秉中

(电子科技大学 物理电子学院,四川 成都 610054)

摘要:在毫米波段,为了更精确、快速地设计出非谐振型低副瓣波导缝隙天线,提出了一种改进型解析方法,具体方法为在传统的斯蒂文生公式引入一个修正因子。该修正因子可大幅度提高波导宽边上的径向缝隙偏移量的解析计算精度。一般情况下,传统斯蒂文生公式仅适用于长宽比大于10∶1的窄缝设计。而此方法则可用于低副瓣、长宽比接近4∶1的宽缝波导缝隙天线的快速设计。对修正公式进行了理论分析,并使用改进型公式,设计加工出了一个工作频率为60 GHz的波导缝隙原型天线,实测增益和副瓣电平分别为14.8 dB和−25 dB。仿真结果以及测试数据吻合良好,证实了此改进型方法的有效性。

关 键 词:毫米波;波导缝隙天线;斯蒂文生公式;泰勒分布

中图分类号:TN92 **文献标识码**:A

Introduction

Slotted Waveguide Antennas (SWAs) date back to World War II and have been very popular from 1940s to now because of their simplicity, high power handling capacity and relatively low profile. A comprehensive review of SWAs is given in references [1-4].

SWAs with low sidelobes, high gain and tilt fan-beams operating in travelling -wave mode has been extensively studied. The design of longitudinal slots in a waveguide can be completed using the moment method or famous Elliot's design equations [5-7]. However, they result in complex formula derivation and burdensome programming and debugging, especially for designing an array of a great number of slots. With rapid development of high performance computers, SWAs can be designed using the field-solver based commercial software like Ansoft HFSS, Feko, and CST Microwave Studio[8]. They are effective methods but need tremendous computing resources for large-aperture millimeter-wave SWA design.

Based on the traditional Stevenson's formula, we

Received date: 2014 - 01 - 21, **revised date**: 2014 - 03 - 13 **收稿日期**:2014 - 01 - 21, **修回日期**:2014 - 03 - 13

Foundation items: Supported by National Natural Foundation of China (61371106, 61331007, 61201089)

Biography: Zhao De-shuang (1974-), female, Henan Xinxian, PhD., Research area involves antennas and propagation, time reversal electromagnetics and applications.

* **Corresponding author**: E-mail: dszhao@uestc.edu.cn

present an improved analytical method for millimeter-wave SWA design in this paper. This method is simpler and faster than the field-solver based numerical methods due to its analytical calculation of the SWA parameters. With the proposed method, a 60-GHz SWA with low sidelobe levels and wide slots was successfully fabricated and demonstrated. Note that in this design mutual coupling effects could be neglected since they are not strong for the end-to-end arranged slots instead of parallel arrangement.

1 Modification of Stevenson formula

Stevenson developed his formulas for representing slot characteristics by making the following assumptions[5-6]:

(1) The walls of the waveguideare perfectly conducting and of negligible thickness;

(2) The width of the slotis much less than its length;

(3) The waveguide transmitted only the TE10 wave, and the length of the slotis nearly equal to $\lambda_0/2$;

(4) The slotis radiating over a perfectly conducting ground plane of infinite extent.

Using transmission line theory and the waveguide modal Green's functions, Stevenson derived the values of the resonant resistance and conductance, normalized to the waveguide impedance, for various slot types along a rectangular waveguide.

For longitudinal shunt slots cut in the broad face of a waveguide, the conductance of the slot is given by[6]:

$$g = g_1 \sin^2\left(\frac{x\pi}{a}\right) \quad , \quad (1)$$

$$g_1 = \frac{2.09a\lambda_g}{b\lambda_0}\cos^2\left(\frac{\lambda\pi}{2\lambda_g}\right) \quad , \quad (2)$$

where λ_0 is the free-space wavelength, λ_g is the guide wavelength, x is the slot displacement from the waveguide centerline, and a, $b$are the waveguide width and height.

Therefore, slot displacement x from centerline is *equal* to[6]:

$$x = \frac{a}{\pi}\arcsin\left(\sqrt{\frac{g}{g_1}}\right) \quad . \quad (3)$$

In millimeter-wave band, due to the strength of the antenna structure and current manufacturing processes, the thickness of the waveguide walls cannot be too thin, typically about 1 mm, which is on the same order of magnitude of the operating wavelength. And the width of the slot cannot be too narrow. Obviously, the first and second of Stevenson's assumption cannot be satisfied for millimeter-wave SWA design. Therefore, for millimeter-wave wide-slot SWAs design, some modifications of Stevenson's formula should be made. Detailed derivation and explanation of Stevenson's formula is given in Ref. [9]. In this paper only some important conclusions are given in the following.

Firstly, according to Booker's relation [10], the radiation resistance R_s of slots cut in an infinite ground plane can be determined by the radiation resistance R_d of the complementary dipole antenna:

$$R_S = \frac{\eta_0^{\ 2}}{4R_d} \quad , \quad (4)$$

where η_0 is the intrinsic impedance of the surrounding medium. For free space, $\eta_0 = 120\pi$. For a slot cut in the waveguide wall, assuming that the waves from the slots only radiate into half of the free space, the radiation conductance will be half of the slot cut in an infinite ground plane. Hence,

$$G_s' = \frac{R_d}{2(60\pi)^2} \quad . \quad (5)$$

Then the conductance of the longitudinal shunt slots cut in the broad face of a waveguide is given by:

$$g = \frac{1}{G'_S\eta_0}\left(\frac{2a}{\pi}\right)^2\frac{4}{ab}\frac{\lambda_g}{\lambda_0}\cos^2\left(\frac{\pi\lambda_0}{2\lambda_g}\right)\sin^2\left(\frac{\pi x}{a}\right) . \quad (6)$$

For an infinitesimally thin slot, the resistance of the complementary dipole antenna is

$$R_d = 73.1 \quad , \quad (7)$$

substituting Eq. (7) into Eq. (6) yields Eq. (1).

Typically, the resistance of the complementary dipole antenna increases as the slot becomes wider. So, the actual conductance of the wide slot is smaller than the value given by Eq. (1). This fact gives some clues to modify the traditional Stevenson's formula. From the above analysis, a scaling factor can be introduced into the Stevenson's formula as follows

$$x = \frac{a}{\pi}\arcsin\left(k\sqrt{\frac{g}{g_1}}\right) \quad , \quad (8)$$

where the scaling factor k is greater than 1. In this paper, the effective range of k will be determined by numerical optimization. Our simulation results show that when the value of the factor k is about 2, the SWA results in good performance.

2 Antenn adesign parameters

The design of any SWAs is an amalgamation of two individual antenna theories: one concerned with the waveguide characteristics and the other with slots and slotted arrays. Waveguide influences the type of wave passing through the structure and frequency at which the antenna operates. The slots influence the manner in which the energy is manipulated.

2.1 Antenna design parameters

As is demonstrated in Fig. 1, a uniformly spaced traveling-wave slot array can be designed to produce a low-sidelobe fan beam pointing the peak of the beam to

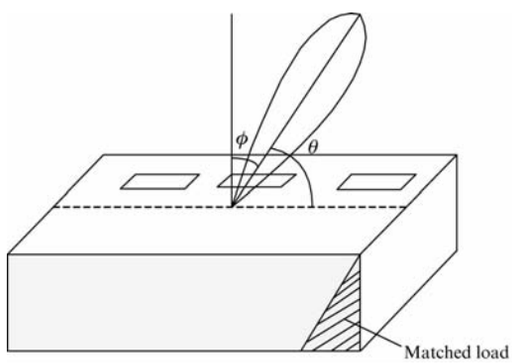

Fig. 1 The relation between antenna beam tilt angle and waveguide dimensions

图1 波导尺寸与天线波束偏转角度关系

angle ϕ. For longitudinal shunt slots cut in the same side of the centerline of the broad face of a waveguide, the relation between the tilt angle and waveguide dimensions can be represented as follows if the reflections between elements are negligible.

$$a = \frac{\lambda_0}{2\sin\theta} \quad , \quad (9)$$

where a is the width of the waveguide. The above formula means that the tilt angle θ is determined by only the width of the waveguide and the free space wavelength. Slot spacing doesn't affect the tilt angle. Thus we can freely choose the slot spacing regardless of the tilt angle. The height b of the waveguide is set to be half of the width.

2.2 Position of the feed and matched load

The position of the feed should be far enough from the center of the first slot, which avoids the influence of the high-order modes near the slot. A matched load terminates the SWAs to prevent the formation of a secondary beam due to reflected waves. Also, the distance between the matched load and the center of the last slot should be far enough.

3 Slots and array design

3.1 Width andlength of slots

The width of the slots is usually determined by

$$\lambda_0/200 \leqslant W \leqslant \lambda_0/10 \quad . \quad (10)$$

However for millimeter-wave SWAs, the width given by Eq. (10) is too narrow. It will be difficult to fabricate. The slots used in the simulations and experiments presented in this paper have an aspect ratio of approximately 4∶1, which makes them become wider and easier for fabrication.

The length of the slots is about $\lambda_0/2$, which is near the resonant length. In fact, the resonant length of the slots is affected by the position of the slots along the waveguide, its displacement from centerline, slot width, and the frequency of operation. This parameter needs to be optimized. In this paper we set the initial value of the length equal to $0.49\lambda_0$.

Analytical methods are most conveniently formulated for rectangular slots. But for fabrication, slots with round ends are used. Therefore, it needs a conversion between rectangular slots and round-end slot. Setting the area of the round-end slot equal to the rectangular slot leads to:

$$L_{round} = L_{rec} + \left(1 - \frac{\pi}{4}\right)W \quad , \quad (11)$$

where L_{round} is the resonant length for round-end slot, L_{rec} is the resonant length for the rectangular slot and W is the slot width.

3.2 Spacing between slot centers

To ensure the SWA with only one main lobe and no grating lobes, the spacing d between slots must be satisfied with the following condition

$$d < \frac{\lambda_0\lambda_g}{\lambda_0 + \lambda_g} \quad . \quad (12)$$

In ourdesign we set to be $0.84\frac{\lambda_0\lambda_g}{\lambda_0 + \lambda_g}$.

3.3 Number of slots and slotted array length

Given the beamwidth and the beam tilt angle, the slotted array length L is determined by

$$L = \sigma\beta_0 \frac{\lambda_0}{\theta_{HPBW}\cos\theta} \quad , \quad (13)$$

where θ_{HPBW} is the HFBW, σ is the Taylor scaling factor, β_0 is the beamwidth factor, θ is the beam tilt angle.

Given the slots spacing and the array length, the number of slots is determined by

$$N = \left[\frac{L}{d}\right] + 1 \quad , \quad (14)$$

where N is the number of slots, [ ] means rounding.

3.4 Taylor taper for array

Taylor taper is adopted in low-sidelobe array design. Chebyshev weighting is practical for a small linear array, but for large array, the amplitude weights at the edge of the aperture increase. Increasing the edge taper brings problems with edge effects and mutual coupling. Taylor taper is similar to the Chebyshev taper but it is suited for large low-sidelobe arrays. The difference is that Taylor taper has the first $\bar{n} - 1$ sidelobes on either side of the main beam at a specified height. All remaining sidelobes decrease at the same rate.

3.5 Conductance determination of slots

Figure 2 shows the equivalent circuit of the SWAs for longitudinal shunt slots cut in the broad face of a waveguide. In the figure g_n represents the equivalent conductance of the slots.

The slot conductance can be computed as follows if the waveguide can be considered as lossless and if the reflection coefficient due to each slot is minimal.

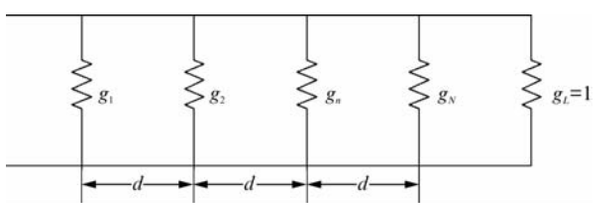

Fig. 2 The equivalent circuit of the SWA
图 2 SWA 的等效电路

$$g_n = \frac{Kp_n}{P_{in} - K\sum_{j=1}^{n-1} p_j} \quad , \quad (15)$$

where P_{in} is the input power to the waveguide; p_j is the normalized power radiated by slot j given by $A^2(j)$, the calculated slot excitation; K is the power calibration factor given by

$$K = \frac{P_{in} - P_L}{\sum_{i=1}^{N} p_i} \quad . \quad (16)$$

For arrays with a large number of slots, the determination of the slot conductance by Eq. (15) is very accurate since the coupling factor is low. However for arrays with fewer slots, the coupling factor is higher, and the slots create impedance mismatches.

3.6 Slot displacement from centerline

In Section 2, we made some modifications to the traditional Stevenson formula for designing millimeter-wave SWAs with wide slots. Therefore, the slot displacement of the SWA in our design will be calculated using the modified formula.

4 Design results

4.1 Determination of the modified factor

Figure 3 depicts the top view of the geometry of the designed SWA. The SWA operates in 60 GHz band. It was designed with the modified Stevenson's formula and numerically validated by Ansoft HFSS. All the thickness of the waveguide wall is set to 1 mm. The beam tilt angle is set to 60 degrees, and the total number of the slots is 21. The final design parameters are shown in Table 1. The variables a, b, L_{round}, W, d are all in unit of mm and have the same meaning as the ones used in Ref. [5,11].

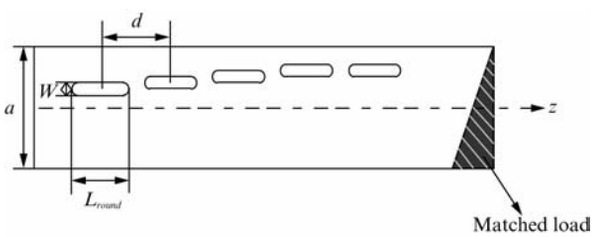

Fig. 3 Top view of geometry of the designed wide-slot low-sidelobe SWA

图3 宽带低副瓣 SWA 的几何结构顶视图

For the slot displacement calculation, firstly we validate the effectiveness of the modification. Simulation experiments and results for a non-resonant SWA consisting of 21 broad-wall slots operating in 60 GHz band determined by different modified factors are given here. A Taylor distribution for side-lobes lower than −35 dB is used in the design. The power absorbed in the load is approximately 4%.

Table 1 Design parameters of SWA

表1 SWA 的设计参数

a	b	L_{round}	W	d
2.887	1.443 5	2.56	0.6	2.7

The radiation patterns obtained by using different modified factor k are shown in Fig. 4. Several conclusions can be obtained from the numerical simulations:

(1) For $k = 1$, the case of no modification, the simulated sidelobes increase compared with the modified ones. It indicates that our modification is effective.

(2) The effective range of the modified factor k for −30 dB sidelobe design is:

$$1.6 \leqslant k \leqslant 2.2$$

(3) When the value of k increases, the beamwidth of the antenna is broadened and the gain of the main lobe decrease. More energy is dispersed in sidelobes.

Based on the numerical validation, we find that $k = 2.0$ is good for the millimeter-wave SWA design.

4.2 Fabricated SWA operating in 60 GHz band

The SWAwas fabricated with aluminum and measured with Agilent Vector Network Analyzer E8361A. Figure 5 shows the photographs of the fabricated antenna. The SWA was fed by a standard WR-14 waveguide from the back side. The transition from the WR-14 waveguide to the SWAs was realized by a vertical transitional waveguide.

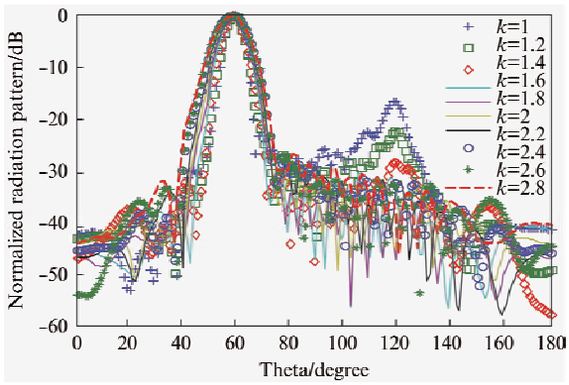

Fig. 4 Normalized radiation patterns obtained by using different k

图4 采用不同 k 值得到的归一化辐射方向图

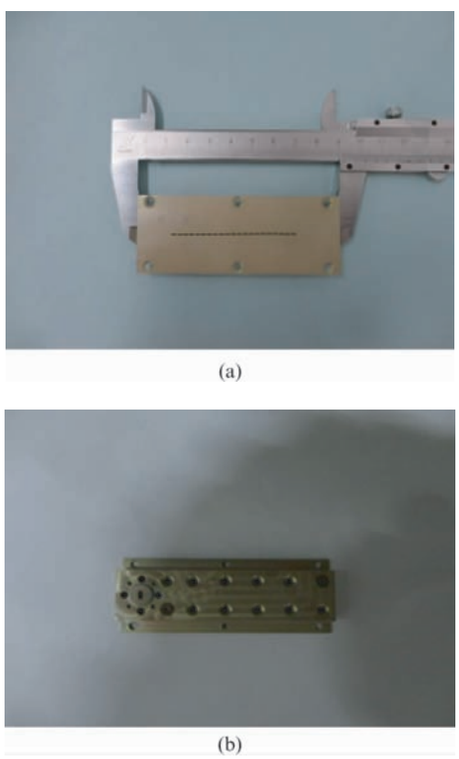

Fig. 5 Photography of the fabricated SWAs. (a) top and (b) bottom views

图5 制作出的 SWA 实物照片.(a) 顶部 和(b)背部

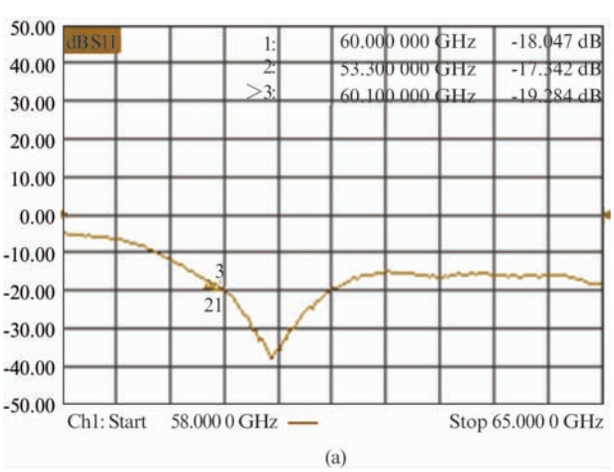

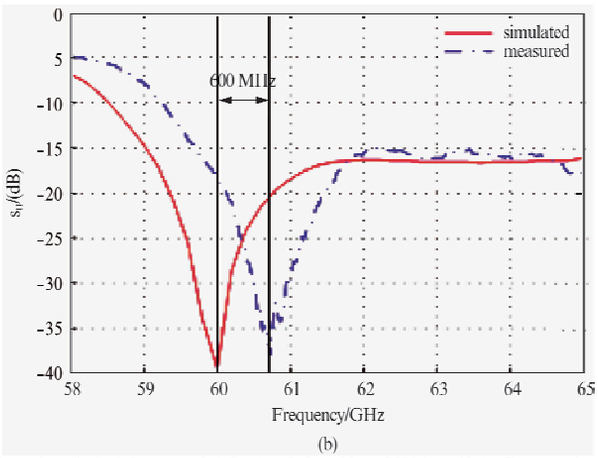

Fig. 6　(a) Measured $|S_{11}|$ of the (b) SWA; (b) Comparison between the measured and simulated $|S_{11}|$ of the SWA

图 6　(a)SWA 的$|S_{11}|$测量值;(b)SWA 的$|S_{11}|$的测量值与仿真值之间的比较

We first measured $|S_{11}|$ of the SWA. Fig. 6 (a) depicts the measured curve. The curve shows that the designed SWA is well matched. The −15 − dB bandwidth is more than 5 GHz. Fig. 6(b) compares the simulated and the measured S_{11}-parameters of the SWA. It can be found from the figures that the measured data agree well with the simulated results. Although the measured operating frequency has a shift of about 600 MHz from the simulated one, we find the relative frequency shift is very small, about 1%. Such frequency shift mainly results from the manufacturing errors, which could be acceptable for most engineering applications.

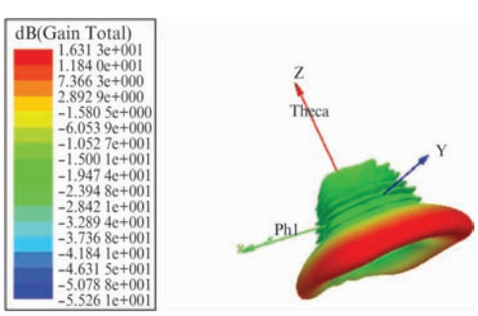

Fig. 7　3D gain patterns at 60 GHz

图 7　在 60 GHz 处的 3D 增益图

Second, we investigate the radiation properties of the SWA. Figure 7 shows the 3D gain patterns obtained by the numerical simulations. As expected, the SWA has a tilt fan beam. Figure 8 compares the measured H-plane pattern of the designed SWA with its simulated one. The measurement of the radiation pattern was performed in the real environment, not in the microwave anechoic chamber. The measured sidelobes are lower than −25 dB. Due to the manufacturing errors and the environment noise, the measured sidelobes are 8 dB higher than the simulated ones. Despite the difference, it is still an effective low-sidelobe design, whose sidelobe is lower than −25 dB. The realized radiation gain of the SWA is 14.8 dB and its efficiency is about 80%. Due to metal losses and load absorption, the measured gain and the measured efficiency are a little less than the ones obtained by the numerical simulations. In simulations, the maximum gain is about 16.3 dB and the simulated efficiency is above 90%.

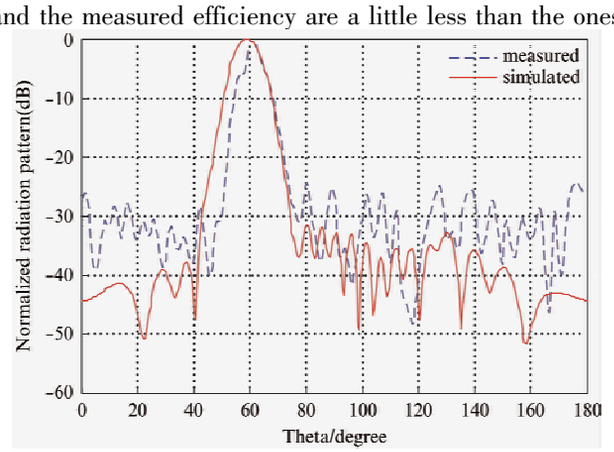

Fig. 8　Comparison between simulated and measured results of H-plane patterns at 60 GHz

图 8　在 60 GHz 处 H 面方向图的测量值与仿真值比较

5　Conclusion

An improved analytical method for millimeter-wave wide-slot low-sidelobe SWA design is successfully developed in this paper by introducing a modified factor into the traditional Stevenson's formula. The traveling-wave SWA operating in 60 GHz band was well designed and measured. The good agreement between simulations and measurements validates the effectiveness of the new method.

References

[1] Hosseininejad S E, Komjani N. Optimum design of traveling-wave SIW slot array antennas [J]. *IEEE Trans. Antennas Propagat.*, 2013,**61**(4):1971 − 1975.

[2] Casula G A, Mazzarella G, Montisci G. Design of shaped beam planar arrays of waveguide longitudinal slots [J]. *International Journal of Antennas and Propagation*, 2013, Article ID 767342.

[3] Xu J F, Hong W. Design and implementation of low-sidelobe substrate integrated waveguide longitudinal slot array antennas [J]. *IET Microw. Antennas Propagat.*, 2009,**3**(5):790 − 797.

[4] Rengarajan R S, Josefsson L G, Elliott R S. Waveguide-fed slot antennas and arrays: A review[J]. *Electromagnetics*, 1999,**19**(1):3 − 22.

[5] Volakis J. Antenna Engineering Handbook [M] *McGraw-Hill Inc.*, New York, 2007,217 − 252.

[6] Elliott R S. An improved design procedure for small arrays of shunt slots [J]. *IEEE Trans. Antennas Propagat.*, 1983, AP-31: 48 − 53.

[7] Haupt R L. Antenna Arrays: A Computational Approach [M]. *John Wiley & Sons*, Hoboken, 2010:127 − 140.

[8] WANG W, ZHONG S. -S. A broadband slotted ridge waveguide antenna array [J]. *IEEE Trans. Antennas Propagat.*, 2006,**54**(8):2416 − 2420.

[9] Gong K, Chen Z. -N. Empirical formula of cavity dominant mode frequency for 60-GHz cavity-backed wide slot antenna [J]. *IEEE Trans. Antennas Propagat.*, 2013,**61**(2):969 − 972.

[10] H. G. Booker. Slot aerials and their relation to complementary wire aerials, JIEE(Lond.), 93,Part. III-A, no. 4, 1946.

[11] YUAN Xian-Gang, YANG Tong-Hui, ZHAO De-Shuang. The design of V-band slotted waveguide antennas with low sidelobes [J]. *Guidance & Fuze*, 2011,**32**(3):29 − 31.